Impedance spectroscopic studies on congruent $LiNbO_3$ single crystal

2007 J. Phys.: Condens. Matter 19 086225

(http://iopscience.iop.org/0953-8984/19/8/086225)

IOP PUBLISHING JOURNAL OF PHYSICS: CONDENSED MATTER

J. Phys.: Condens. Matter **19** (2007) 086225 (10pp) doi:10.1088/0953-8984/19/8/086225

Impedance spectroscopic studies on congruent $LiNbO_3$ single crystal

R H Chen[1], **Li-Fang Chen and Chih-Ta Chia**

Department of Physics, National Taiwan Normal University, 88, Section 4 Ting-Chou Road, Taipei 11677, Taiwan

E-mail: rhchen@phy03.phy.ntnu.edu.tw

Received 4 August 2006, in final form 22 December 2006
Published 9 February 2007
Online at stacks.iop.org/JPhysCM/19/086225

Abstract

Electrical impedance measurements on a congruent $LiNbO_3$ single crystal were performed as a function of both temperature and frequency. The measurements were carried out in the directions along the *c*- and *a*-axes of the crystal. The temperature and frequency dependence of various dielectric properties have been studied. The result has revealed two remarkable dynamic relaxations: dielectric dipolar relaxation and ionic conductivity relaxation. The dipolar relaxation peaks were found at frequencies around 4×10^6 and 2×10^6 Hz for the *c*-axis and *a*-axis, respectively, and they were only slightly temperature dependent. The ionic conductivity relaxation was found at the lower-frequency end but it was temperature dependent. The temperature dependence of the dc electrical conductivity follows the Arrhenius law. It corresponds to the long-range ionic motion of Li^+ ions which are thermally activated with activation energy of 0.90 and 0.87 eV along the *c*- and *a*-axis directions, respectively. The dc conductivities measured along the *c*- and *a*-axes are very close to each other, and the value increases from 1.7×10^{-6} to 1.9×10^{-3} Ω^{-1} cm^{-1} as the temperature is raised from 300 to 700 °C. The sample crystal becomes an ionic conductor as the temperature is raised.

1. Introduction

$LiNbO_3$ is a well known ferroelectric material and it is used widely in nonlinear optics devices. $LiNbO_3$ crystal is a typical displacive-type ferroelectric with very high Curie temperature of 1210 °C [1]. The crystal structure of $LiNbO_3$ in the ferroelectric phase belongs to the $R3c$ space group, where Li^+ and Nb^+ ions occupy the hollows of oxygen octahedra with the sequence of cations . . .–Li–Nb–□–Li–Nb–□–Li–. . . along the triad axis [2]. The polarity of $LiNbO_3$ was confirmed by the existence of piezo- and pyro-electric effects at room temperature [3]. The

[1] Author to whom any correspondence should be addressed.

high Curie temperature is typical for octahedral oxygen compounds and this is assumed to be associated with the greater polarizability of the oxygen octahedron with niobium. $LiNbO_3$ is generally grown from a congruent melt. A considerable deficiency of lithium ions was present in the congruent $LiNbO_3$ crystal. There have been many studies of the defect model of $LiNbO_3$ crystal in the past decades, but which model gives the best description is still an open question. Possible intrinsic defect models have been proposed. The most frequently concerned models are the Li-vacancy [4], Nb-vacancy [5], and O-vacancy models [6]. The first two models are that each missing Li^+ ion at Li sites is replaced by a Nb^{5+} ion, with compensating vacancies at lithium sites (V_{Li}^{1+}) or at the niobium site (V_{Nb}^{1+}) to maintain charge neutrality. The less favoured O-vacancy model is that the compensating vacancies are created at oxygen sites.

The electrical properties of lithium niobate at certain fixed frequencies have been investigated by many researchers [1, 7–12]. The long-range hopping of Li^+ or polaron formation has been adopted to account for the conduction in their studies. Mansingh and Dhar measured the ac conductivity and dielectric constant of lithium niobate single crystal at some frequencies below 100 kHz in the temperature range between 77 and 700 K [9]. Recently, impedance measurements on different forms of $LiNbO_3$ samples (such as polycrystalline ceramics, wafers, nanocrystalline, and amorphous) have been carried out [10–12]. Although a frequency up to 13 MHz was used, a complete analysis of the frequency dependence of the dielectric properties for lithium niobate single crystal has not been given.

In this work, we present studies of the dielectric properties of a congruent $LiNbO_3$ single crystal using the ac-impedance spectra, measured over a wide range of frequency (100 Hz–40 MHz) and with the temperature controlled between 150 and 700 °C. In this wide range of frequency, different polarization dynamic processes are analysed. The temperature and frequency dependences of dielectric relaxation and electrical conduction for a congruent $LiNbO_3$ crystal were investigated.

2. Experimental details

The $LiNbO_3$ single crystals were grown from a congruent melt ($[Li]/([Li] + [Nb]) = 0.486$) according to the Czochralski method. The sample crystals were cut in the directions parallel or perpendicular to the polar *c*-axis. The sample crystals were coated with silver paste on the plate surface.

Complex impedance measurements were carried out using an HP4194A impedance analyser in the frequency range between 100 Hz and 40 MHz. The temperature of the sample crystal was controlled from 150 to 700 °C in an atmosphere of normal laboratory air. These temperatures are well below the Curie temperature. Below 150 °C, the impedance of the sample crystal was too large to be measured accurately. The temperature increment between each set of measurement was 50 °C, and this was controlled with the stability ±0.5 °C.

3. Results and discussion

Various dielectric functions have been used to investigate the dielectric properties of a material. Among them are the complex impedance ($Z^*(\omega)$), the complex permittivity ($\epsilon^*(\omega)$), the complex admittance ($Y^*(\omega)$), and the complex electric modulus ($M^*(\omega)$). They are in turn related to one another as follows:

$$Z^*(\omega) = Z'(\omega) - \mathrm{i}Z''(\omega), \tag{1}$$

$$\epsilon^*(\omega) = \epsilon'(\omega) - \mathrm{i}\epsilon''(\omega) = \frac{1}{\mathrm{i}\omega C_0 Z^*(\omega)}, \tag{2}$$

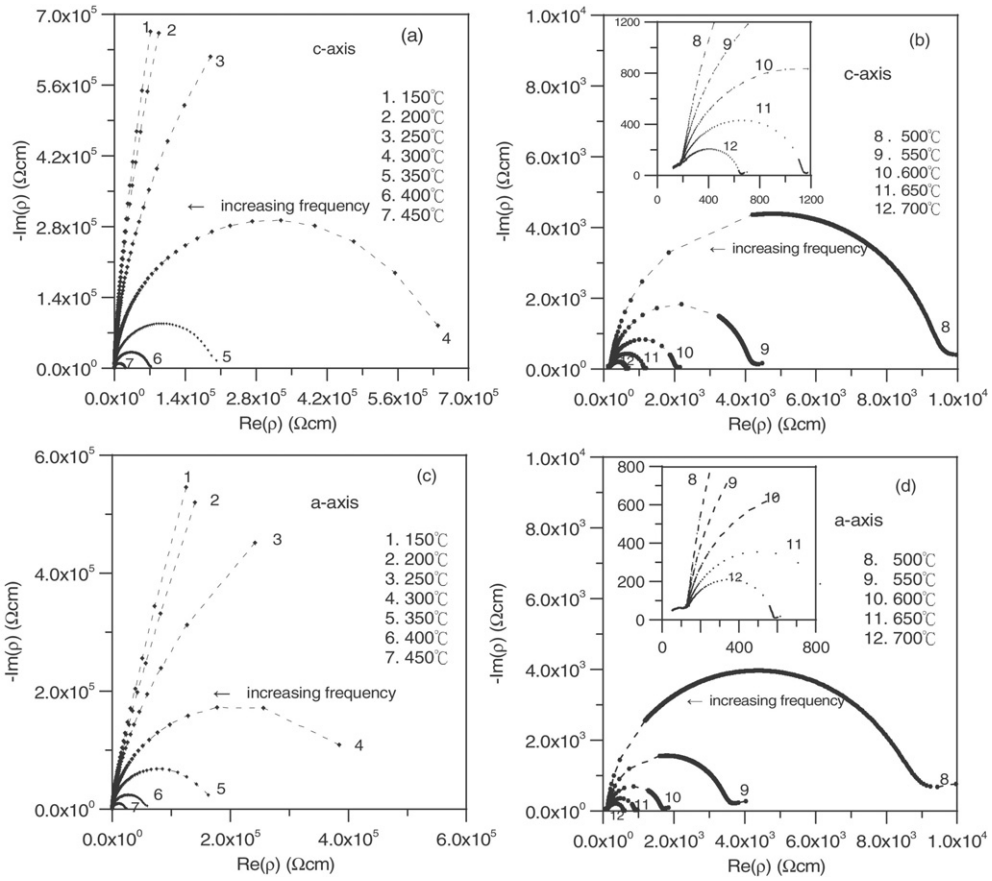

Figure 1. The complex resistivity diagrams for a congruent $LiNbO_3$ single crystal at several temperatures as measured in different crystallographic directions. The insets in (b) and (d) are the enlargement of the high-frequency end.

$$Y^*(\omega) = Y'(\omega) + \mathrm{i}Y''(\omega) = \frac{1}{Z^*(\omega)} = \mathrm{i}\omega C_0 \epsilon^*(\omega), \tag{3}$$

and

$$M^*(\omega) = M'(\omega) + \mathrm{i}M''(\omega) = \frac{1}{\epsilon^*(\omega)}, \tag{4}$$

where $\mathrm{i} = \sqrt{-1}$, ω is the external ac field frequency, and C_0 is the capacitance of the sample in vacuum. Sometimes the complex resistivity $\rho^*(\omega)$ $(=\frac{A}{t}Z^*(\omega))$ and complex conductivity $\sigma^*(\omega)$ $(=\frac{A}{t}Y^*(\omega))$ are used to get rid of the geometrical factors of the sample with its area A and thickness t. A different representation is chosen to extract the different relevant parameters. All the relevant effects might be well separated if the range of the applied ac frequency wide enough to cover the studied range.

The analysis of ac complex dielectric spectra is often carried out by complex plane method, which involves plotting the imaginary part against the real part, i.e. the Cole–Cole Plot. The complex resistivity of the sample crystals was evaluated from the measured complex impedance. Figures 1(a) and (b) show the resistivity Cole–Cole plots of the $LiNbO_3$ sample crystal obtained for the measurements along the c-direction at several temperatures.

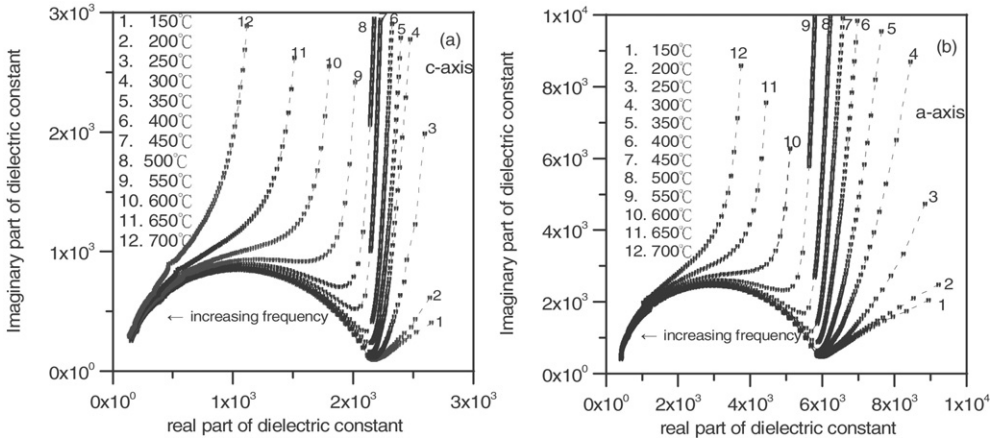

Figure 2. The complex permittivity diagrams for a congruent $LiNbO_3$ single crystal at several temperatures measured in different crystallographic directions.

Semicircles were obtained. But some of the semicircles are incomplete, especially at temperatures below 250 °C. This is because the resistivity of the sample crystal is very large at low temperatures and also the measurements at the low-frequency end are limited by the HP4194A impedance analyser. As the temperature is raised, the semicircles become smaller. This indicates that the resistance of the crystal decreases with the increasing temperature. An inclined spike also appeared at the low-frequency end. This indicates that the mobile ion has a surface electrode effect especially at higher temperatures. The electrode effect usually appears at the relatively low-frequency end. It is a typical effect of an ionic conductor and it suggested that the mobile charge carriers are ions which are blocking the metal–sample interface. A relatively small incomplete semicircle was also observed at the high-frequency end, as shown in the inset. This portion is due to the dipolar response of the sample crystal. Figures 1(c) and (d) show the results measured in the direction perpendicular to the *c*-axis at various temperatures. The variation of the impedance spectrum with frequency is similar to that along the *c*-axis. But the radii of the semicircles obtained in this direction are slightly smaller than those along the *c*-axis at the same temperature.

The dielectric constant ϵ^* were converted from the measured impedance data according to equation (2). Figures 2(a) and (b) shows the dielectric constant Cole–Cole plots obtained for measurements along the *c*-axis and *a*-axis, respectively. An almost complete semicircle was obtained for lower temperatures. The contribution of this part is due to the response of the dipoles in the sample and can be explained well by the Debye model. The additional spike was added at the low-frequency end for low temperatures and this became the vertical line which extended quickly to become very large for higher temperatures. This part is attributed to the mobile ions. The electric response of a material to an external electric field includes many possible polarization mechanisms. From the results shown in figures 1 and 2, the electric response of the sample crystal to the external field contained two main contributions: one is the dipolar orientation and the other one is the long-range motion of ions.

If the electric response of the sample contains dipolar reorientation and a long range of ionic motion as mentioned above, the sample in the measuring circuit can be treated as an r–C_s series in parallel with R and C_∞, where r is the resistance due to the orientation of dipoles in the sample, C_s is the static capacitance due to the reorientation of dipoles, R is the dc resistance of long-range mobile ions, and C_∞ represents the permittivity when the frequency ω

approaches infinity [13]. Based on this model, it can be shown that the frequency dependence of the complex permittivity, $\epsilon^*(\omega)$, of the bulk is described as follows:

$$\epsilon^*(\omega) = \epsilon^*(\omega)_{\mathrm{D}} + \epsilon^*(\omega)_{\mathrm{C}}, \tag{5}$$

where $\epsilon^*(\omega)_{\mathrm{D}}$ is the permittivity due to the dipolar response, and $\epsilon^*(\omega)_{\mathrm{C}}$ is the permittivity due to long-range migration of charge carriers. It is the linear combination of two contributions. It can also be shown by straightforward mathematics that the real and imaginary parts of $\epsilon^*(\omega)$ have the following form:

$$\epsilon'(\omega) = \epsilon_\infty + \epsilon'_{\mathrm{D}}(\omega) = \frac{t}{\epsilon_0 A}\left[C_\infty + \frac{C_{\mathrm{s}}}{(1+\omega^2 r^2 C_{\mathrm{s}}^2)}\right] \tag{6}$$

and

$$\epsilon''(\omega) = \epsilon''_{\mathrm{D}}(\omega) + \epsilon''_{\mathrm{C}}(\omega) = \frac{t}{\epsilon_0 A}\left[\frac{\omega r C_{\mathrm{s}}^2}{(1+\omega^2 r^2 C_{\mathrm{s}}^2)} + \frac{1}{(\omega R)}\right]. \tag{7}$$

where ϵ_0 is the free space permittivity, ϵ_∞ is the high-frequency limit of the permittivity, C_{s} is the static capacitance due to the reorientation of dipoles, and C_∞ represents the capacitance when the ac frequency approaches infinity.

The evolutions of the real part of permittivity with the frequency for both axes of a congruent $LiNbO_3$ single crystal are shown in figures 3(a) and (c). These show that the dielectric constant increases rapidly with decreasing frequency for temperatures higher than 400 °C. The effect is attributed to two factors: one is the increasing conduction contribution from mobile ions and the other is the effect of the electrode polarization. The variation of the dielectric constant is slightly decreasing with increasing frequency in the frequency range between 3×10^4 and 2×10^6 Hz. The dielectric constants are around 2×10^3 and 5–8.5×10^3 for the *c*-axis and *a*-axis, respectively. This shows that the polarization due to the orientation of the diploes in a congruent $LiNbO_3$ single crystal is relatively easier along the *a*-axis than that along the *c*-axis. However, the values dropped quickly to 153 for the *c*-axis and 420 for the *a*-axis at 4×10^7 Hz for most temperatures. The frequency evolutions of the imaginary part of the permittivity for the *c*-axis and the *a*-axis are also shown in figures 3(b) and (d), respectively. Each curve contains two parts, as described in equation (7). One, with ω^{-1} frequency dependence, is due to the conduction contribution at the low-frequency end and the other, with a peak around 10^6 Hz, is due to the contribution of dipoles. The first part is increasing with increasing temperature. For the second part in the high-frequency regime, the variations of ϵ' and ϵ'' with frequency are clearly a typical relaxation form. The frequency of the relaxation peaks ω_{D} found at 10^6–10^7 Hz characterizes the typical timescale of the dynamical reorientation of the dipole in a solid.

By subtracting the conduction part, the frequency dependence of the dipolar contribution $\epsilon''_{\mathrm{D}}(\omega)$ for several temperatures is shown in figures 4(a) and (b). The peak positions ω_{D} are almost temperature independent at temperatures below 500 °C, but shift slightly towards the high-frequency end as the temperature is raised. The dielectric relaxation time at each temperature, τ_{D}, is determined by the position of peak and obtained by the relation $\omega_{\mathrm{D}}\tau_{\mathrm{D}} = 1$. The values are determined to be 2.5×10^{-7} and 5×10^{-7} s for the measurements along the *c*-axis and *a*-axis, respectively.

The frequency variations of the real part of the ac conductivity at several temperatures for the two directions are shown in figure 5. The measured conductivity showed a frequency-independent part at the low-frequency end and this is followed by a frequency-dependent part at higher frequencies. The result also showed that the frequency-dependent of the real part of the conductivity is stronger at low temperatures than that at higher temperatures. The

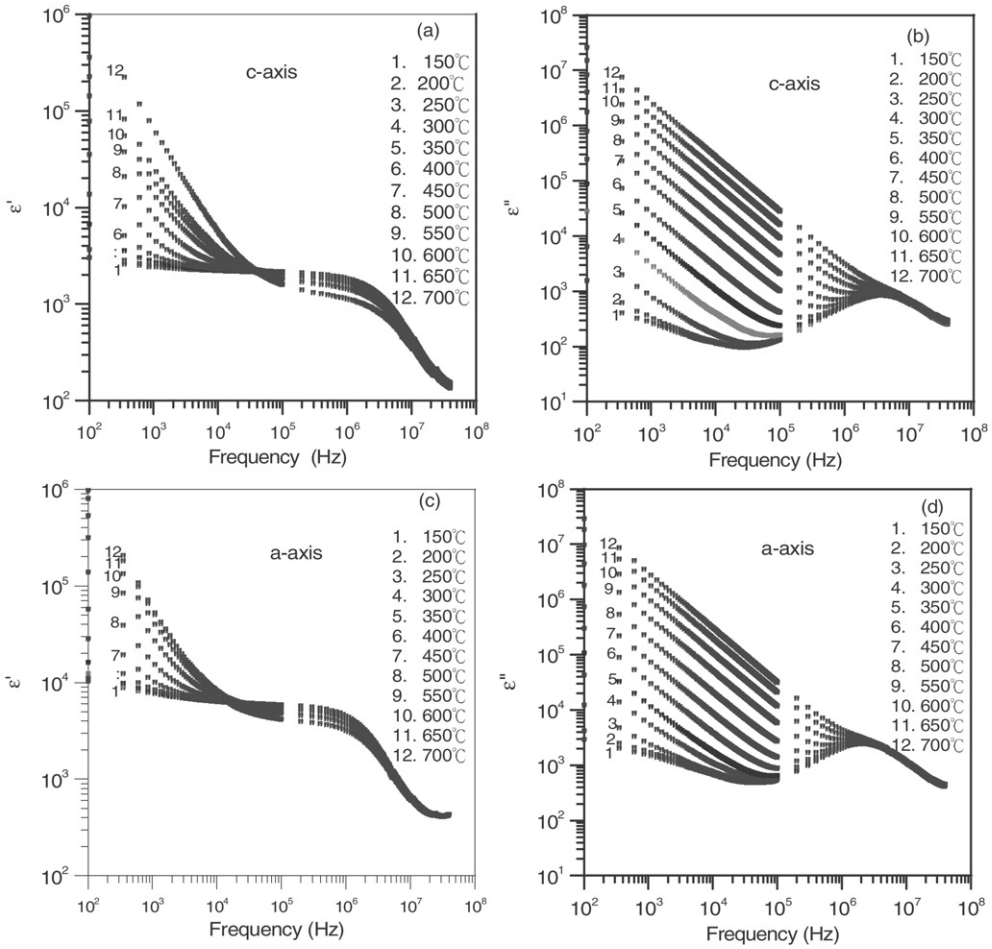

Figure 3. Frequency variations of the real parts (a) and (c), and the imaginary parts (b) and (d) of the dielectric constant for a congruent $LiNbO_3$ single crystal at various temperatures for two different directions.

conductivity increases with increasing temperature. The conductivities all approached a value around $7 \times 10^{-3}\ \Omega^{-1}\ \mathrm{cm}^{-1}$ at a frequency near 10^7 Hz for all temperatures.

The frequency dependence part of the ac conductivity is generally described by Jonscher's power law [14]:

$$\sigma'(\omega) = \sigma(0) + B\omega^{s} \tag{8}$$

where $\sigma(0)$ is the dc conductivity of the sample at a temperature T, and B and s are characteristic parameters. It has been applied not only to glass and amorphous semiconductors, but also to single crystals to analyse the ac conductivity [15–24]. The dc conductivity is due to the long-range movement of free charges. The frequency dependence is usually explained by a hopping conduction mechanism. The exponent s is the measure of the degree of interaction of hopping charged particles with the environment. It is usually temperature and frequency dependent and lies in the range $0 < s < 1$ for most glasses and amorphous semiconductors [17, 25, 26]. For an ideally ionic conductor with free mobile charges, the real part of the ac conductivity is frequency independent; hence s equals zero. Jonscher's power

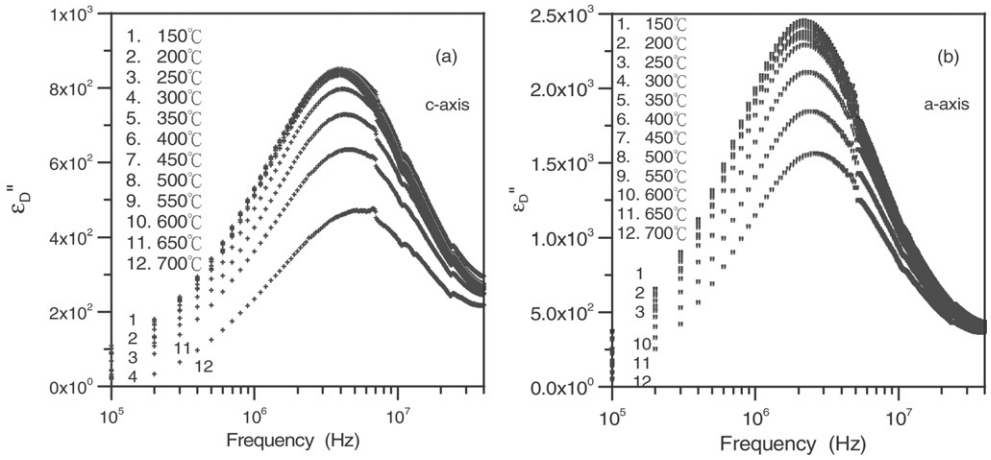

Figure 4. Frequency variation of the imaginary part of the complex permittivity due to the contribution of dipolar relaxation in a congruent $LiNbO_3$ single crystal for two directions at several temperatures.

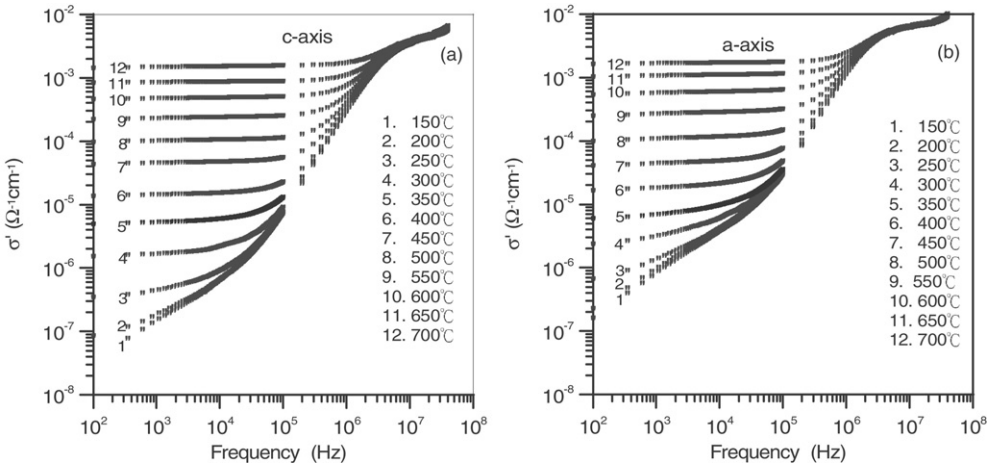

Figure 5. The variation of conductivity with frequency over the temperature range 150–700 °C for two directions in a congruent $LiNbO_3$ single crystal.

law is also referred to as the 'universal dielectric response', showing up as a sublinear power law in the frequency-dependent conductivity. However, the s-values obtained in the present studied samples are 1.3 and 1.2 for the c-axis and a-axis, respectively, at low temperatures. They decrease slightly with increasing temperature. A superlinear power law with $s > 1$ but significantly smaller than 2 has been found on many materials [20, 23, 24, 27–29]. At higher temperatures, the real part of the ac conductivity of the sample crystal is nearly frequency independent for frequencies up to 10^6 Hz. In this frequency region, the mobile ions have made main contribution to the electrical conductivity.

The complex electric modulus of the sample is often used, and it has an advantage in analysing the dynamic relaxation property of sample. It gives the main response of the bulk and eliminates the response of surface electrode effectively [30, 31]. For this expression, both M' and $M'' \rightarrow 0$ as $\omega \rightarrow 0$, while $M' \rightarrow M'_\infty (=1/\epsilon_\infty)$ and $M'' \rightarrow 0$ as $\omega \rightarrow \infty$. M'_∞

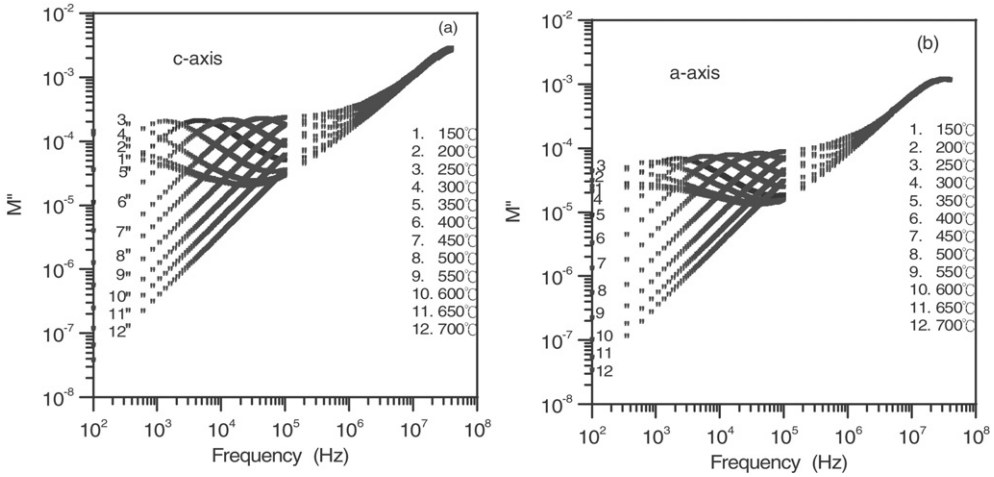

Figure 6. Frequency dependence of the imaginary parts of electric modulus for a congruent $LiNbO_3$ single crystal for two directions at several temperatures.

contains all the contributions of electronic and atomic polarization in the sample crystal. The frequency variation of the imaginary part M'' will reveal the different relaxation processes which take place in the sample and these will be shown up by the peaks related to them. The variations of the imaginary parts of the electric modulus with frequency at several temperatures for a congruent $LiNbO_3$ sample crystal are shown in figure 6. The complete peak at the low-frequency end corresponds to the electrical response of the long-range motion of Li^{+1}. The frequency found for the peak at a given temperature is identified as ω_m. It is related to the conductivity relaxation time τ_m by the relation $\omega_m \tau_m = 1$. As the temperature is raised, the conduction peak ω_m shifts towards higher frequency. The temperature variation of the conductivity relaxation time obtained is plotted in figure 7. It is well described by the Arrhenius relation $\tau_m(T) = \tau_0 \exp(E_M/(k_B T))$, where τ_0 is the pre-exponential factor, E_M is the activation energy for conductivity relaxation, and k_B is Boltzmann's constant. The activation energy E_M obtained from the fitting is 0.87 and 0.78 eV for the c-axis and a-axis, respectively. These values are close to the value of 0.88 eV for an amorphous sample reported by Masoud and Heitjans [12]. The pre-exponential factors τ_0 from the fitting are around 3×10^{10} Hz for the c-axis and 3×10^{11} Hz for the a-axis. They are close to the phonon frequency.

The dc resistivity of the sample crystal was extracted from the resistivity Cole–Cole plot to zero frequency. The conductivity is $1.7 \times 10^{-6}\ \Omega^{-1}\ cm^{-1}$ at 300 °C and it increases to $1.9 \times 10^{-3}\ \Omega^{-1}\ cm^{-1}$ at 700 °C, independent of the direction. Masoud and Heitjans [12] have reported that the ionic conductivity of $LiNbO_3$ was found to increase by going from the single crystal through to the microcrystalline, nanocrystalline and amorphous forms. The conductivity of the congruent $LiNbO_3$ found in this studies is about the same order of magnitude as that of nanocrystalline and amorphous $LiNbO_3$. The temperature variations of dc conductivity ($\log \sigma_{dc} T$ versus $1000/T$) along two directions are also shown in figure 7. A generally accepted form of the Arrhenius relation is also obeyed over the temperature range between 300 and 700 °C. The dc activation energy, E_σ, is 0.90 eV along the c-axis and 0.87 eV along the a-axis at temperatures above 300 °C. These values are slightly higher than the conductivity relaxation activation energies. This is because the activation energy determined from dc conductivity contains two components: one is the ion migration energy, while the other is the intrinsic

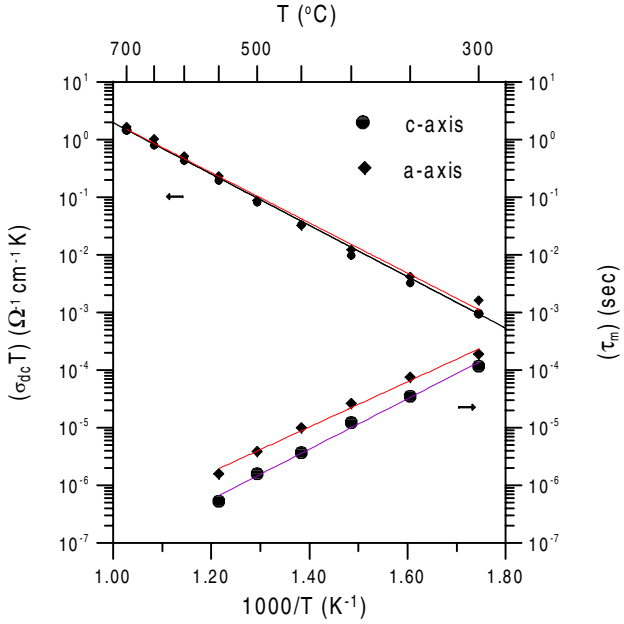

Figure 7. Temperature dependences of the electrical conductivity and the conductivity relaxation time τ_m as measured along the two different directions in a congruent $LiNbO_3$ single crystal. The straight lines are the fits of the Arrhenius relation.

(This figure is in colour only in the electronic version)

defect formation energy. As the temperature increases, the defects are thermally activated and the mobility of the lithium ion is facilitated. It is suggested that the long-range motion of Li^{+1} is hopping between the increasing number of vacancies as the temperature is raised. The dc activation energy found in this study is less than the values found for $LiNbO_3$ ceramic, wafer sample, and single-crystal samples [10–12]. It is close to the value of 0.93 eV for a microcrystalline sample measured by Masoud and Heitjans [12]. It is also close to the value of 1.10 eV obtained on a $LiTaO_3$ crystal which is isostructural with the sample crystal [32, 33].

There is another incomplete peak which appears at $\omega > 10^7$ Hz, as shown in figure 6. It would be due to dielectric dipolar relaxation. It will correspond to the peak observed in the permittivity spectrum as shown in figures 3(b) and (d). However, the peak of this relaxation process will be located at a higher frequency in the electric modulus representation [34]. However, the high-frequency data cannot be obtained by the high limit of the HP4194A impedance analyser.

4. Conclusions

The electrical conduction and dielectric relaxation of a congruent $LiNbO_3$ single crystal have been studied. The impedance data revealed two dynamic responses on the sample crystal: the dipolar dielectric response and the mobile charge carrier response. The conductivity relaxation at the low-frequency end is due to the long-range motion of lithium ions which are thermally activated. The congruently grown lithium niobate single crystal presents a large LiO_2 deficiency; therefore, it contains a lot of intrinsic defects (such as antisite defects of Nb_{Li}^{4+}, V_{Li}^{1+} site vacancies, and V_{Nb}^{1+} site vacancies) [35]. The electrical conductivity of the sample crystal

is related to the hopping of lithium ion among these vacancies. The frequency of a Debye-type dipolar relaxation has been found at around 4×10^6 and 2×10^6 Hz along the c-axis and a-axis, respectively. The dielectric constant measured at 40 MHz along the c-axis and a-axis of the congruent $LiNbO_3$ single crystal in this study is 153 and 420, respectively. It is reasonable that these values are larger than the values reported at 1.0 GHz, which were 25.1 and 45.6 for the c-axis and a-axis, respectively, at 150 °C [36]. The sample crystal becomes an ionic conductor as the temperature is raised.

Acknowledgments

We are grateful to Dr L C Ho for growing the crystals. This work was supported by the National Science Council, Taiwan (Project Nos NSC93-2112-M-003-013 and NSC94-2112-M-003-009).

References

[1] Nassau K, Levinstein H J and Loiacomo G M 1966 *J. Phys. Chem. Solids* **27** 989
[2] Shiosaki Y and Mitsui T 1963 *J. Phys. Chem. Solids* **24** 1057
[3] Peterson Y E, Ballman A A, Lenzo P V and Pridenbaugh P M 1964 *Appl. Phys. Lett.* **5** 62
[4] Lerner P, Legras E and Dumas J P 1968 *J. Cryst. Growth* **3/4** 231
[5] Peterson G E and Carnevale A 1972 *J. Chem. Phys.* **56** 4848
[6] Fay H, Alford W J and Dess H M 1968 *Appl. Phys. Lett.* **12** 89
[7] Bollmann W and Gernand M 1972 *Phys. Status Solidi* A **9** 301
[8] Xi Y, McKinstry H and Cross L E 1983 *J. Am. Ceram. Soc.* **66** 637
[9] Mansingh A and Dhar A 1985 *J. Phys. D: Appl. Phys.* **18** 2059
[10] Lanfredi S and Rodrigues A C M 1999 *J. Appl. Phys.* **86** 2215
[11] Niitsu G T, Nagata H and Rodrigues A C M 2004 *J. Appl. Phys.* **95** 3116
[12] Masoud M and Heitjans P 2005 *Defect Diffusion Forum* **237–240** 1016
[13] MacDonald J R 1987 *Impedance Spectroscopy* (New York: Wiley–Interscience)
[14] Jonscher A K 1983 *Dielectric Relaxation in Solids* (London: Chelsea Dielectrics Press) pp 63–115
[15] Funke K 1993 *Prog. Solid State Chem.* **22** 111
[16] Jain H and Mundy J N 1987 *J. Non-Cryst. Solids* **91** 315
[17] Mott N F and Davis E A 1970 *Electronic Progresses in Non-crystalline Solids* (Oxford: Clarendon)
[18] Dyre J C and Schroder T B 2000 *Rev. Mod. Phys.* **72** 873
[19] Elliott S R 1988 *Solid State Ion.* **27** 131
[20] Chen R H, Wang R-J, Chen T M and Shern C S 2000 *J. Phys. Chem. Solids* **61** 519
[21] Chen R H, Chen T M and Shern C S 2000 *J. Phys. Chem. Solids* **61** 1399
[22] Chen R H, Shern C S and Fukami T 2002 *J. Phys. Chem. Solids* **63** 203
[23] Chen R H, Chang R Y and Shern C S 2002 *J. Phys. Chem. Solids* **63** 2069
[24] Chen R H, Chang R Y, Shern C S and Fukami T 2003 *J. Phys. Chem. Solids* **64** 553
[25] Dyre J C 1988 *J. Appl. Phys.* **64** 2456
[26] Maass P, Meyer M and Bunde A 1995 *Phys. Rev.* B **51** 8164
[27] Ritus A I *et al* 2002 *Phys. Rev.* B **65** 165209
[28] Lunkenheimer P, Pimenov A and Loidl A 1997 *Phys. Rev. Lett.* **78** 2995
[29] Lunkenheimer P and Loidl A 2003 *Phys. Rev. Lett.* **91** 207601
[30] Ambrus J H, Moynihan C T and Marcedo P B 1972 *J. Phys. Chem.* **76** 3287
[31] Macedo P B, Moynihan C T and Bose R 1972 *Phys. Chem. Glasses* **13** 171
[32] Ming D, Reau J M, Ravez J, Gitae J and Hagenmuller P 1995 *J. Solid State Chem.* **116** 185
[33] Abrahams S C, Buehler E, Hamilton W C and Laplaca S J 1973 *J. Phys. Chem. Solids* **34** 521
[34] Gerhardt R 1994 *J. Phys. Chem. Solids* **55** 1491
[35] Watanabe Y, Sota T, Suzuki K, Iyi N, Kitttamura K and Kimura S 1995 *J. Phys.: Condens. Matter* **7** 3627
[36] Teague J R, Rice R R and Gerson R 1975 *J. Appl. Phys.* **46** 2864